Research Article

For reprint orders, please contact: reprints@futuremedicine.com

Nanomedicine

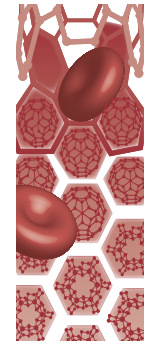

Hybrid core shell nanoparticles entrapping Gd-DTPA and ^{18}F-FDG for simultaneous PET/MRI acquisitions

Aim: Although there has been an improvement in the hardware and software of the PET/MRI system, the development of the nanoprobes exploiting the simultaneous acquisition of the bimodal data is still under investigation. Moreover, few studies on biocompatible and clinically relevant probes are available. This work presents a core-shell polymeric nanocarrier with improved relaxometric properties for simultaneous PET/MRI acquisitions. **Materials & methods:** Core-shell nanoparticles entrapping the Gd-DTPA and ^{18}F-FDG are obtained by a complex coacervation. **Results & discussion:** The boosting of r_1 of the entrapped Gd-DTPA up to five-times compared with 'free Gd-DTPA', is confirmed by the PET/MRI scan. The sorption of ^{18}F-FDG into the nanoparticles is studied and designed to be integrated downstream for the production of the tracer.

First draft submitted: 31 March 2017; Accepted for publication: 3 July 2017; Published online: 17 August 2017

Keywords: dual imaging • nanoparticles • PET/MRI

Donatella Vecchione[1,2], Marco Aiello[3], Carlo Cavaliere[3], Emanuele Nicolai[3], Paolo Antonio Netti[1,2,4] & Enza Torino*[,1,4]

[1]Istituto Italiano di Tecnologia, Center for Advanced Biomaterials for Health Care IIT@CRIB, Largo Barsanti e Matteucci 53, 80125 Naples, Italy

[2]Department of Chemical, Materials & Industrial Production Engineering, University of Naples Federico II, P.le Tecchio 80, 80125 Naples, Italy

[3]IRCSS SDN, Via E. Gianturco 113, 80143 Naples, Italy

[4]Interdisciplinary Research Center of Biomaterials, University of Naples Federico II, CRIB P.le Tecchio 80, 80125 Naples, Italy

*Author for correspondence:
Tel: + 39 081 199 33 100
enza.torino@iit.it

Nowadays, the combination of several imaging modalities is used to increase the diagnostic accuracy. Furthermore, the integration of the imaging modalities enabling the simultaneous acquisition of the different data could have a huge impact in the early diagnosis of various pathologies as neurodegeneration diseases [1–8] and, therefore, in the clinical management of cognitive decline in early stage. In this context a pivotal role is represented by the hybrid PET/MRI [9]; the development of integrated PET/MRI started in 1997 with the aim to acquire simultaneously both modalities combining their diagnostic contribution in a single high-resolution image [9]. Among several other advantages, the guarantee of having, for example, in a single image PET/MRI a high anatomical detail and the information on the metabolic processes associated with a disease not only leads to saving time and money but also gives the opportunity to make an early detection [10] and so to improve the effectiveness of the treatments [11]. Currently, magnetic resonance imaging and positron emission tomography are used separately and, only later, the two obtained images are superimposed on a unique diagnostic image. This implies a high risk of artifacts and the reduction of image resolution due to partial volume effects [12]. So, simultaneously PET/MRI allows for both spatial and temporal correlation of the signals, creating opportunities impossible to realize using sequentially acquired data [13]. The features of this new technology may be particularly appealing to applications in neuroscience [7,13] and translational neurologic and psychiatric research [14], considering that MRI represents the first-line diagnostic imaging modality for numerous indications and that a significant number of specific PET tracers are available today to assess functional and molecular processes [15]. Nowadays, even though there are different commercial contrast agents and radiotracers, there is not a single probe that can be used for the simultaneous PET/MRI acquisition and the only way to exploit this technique is limited to the administration of

Future Medicine part of fsg

a risky cocktail of tracers [16]. Thanks to nanotechnologies, the design of new probes that provide the delivery of drugs and the combination of different molecular targeting is possible [17,18]. The development of an efficient and reliable PET/MR dual imaging probe is essential to actualize the PET/MR instrument's powerful application. Therefore, a dual probe allows an actual simultaneous acquisition and the co-localization of the two contrast agents and guarantees a temporal and spatial correlation of the two imaging modalities. *In vivo*, the probe concentration that is, in general, unknown, will change with time and may vary in diseased versus normal tissue. Using a bimodal PET/MR probe, it has proven suitable to use PET for estimating the overall concentration and the MR signal to determine the molar relaxivity of the agent, giving an accurate estimation of its specific biochemical or physiologic target [19].

In this perspective, several efforts are made to present multimodal probes for PET/MRI [20–24]. However, most of them are mainly based on the bioconjugation of the tracers to a carrier inducing the chemical modification of the molecules as approved for clinical use by the US FDA [25,26] or entrap the diagnostic compounds using not completely biocompatible materials [18,22,27,28]. Lee *et al.* [29] in 2008 presented a study in which arginine-glycine-aspartic (RGD) was conjugated to iron oxide NPs to develop a PET/MRI probe for the detection of tumor integrin $\alpha_v\beta_3$. Hwang *et al.* [30] in 2010, presented a review in which is reported state of the art about the development of new nanoprobe for PET/MRI acquisitions. In 2010, Zhu *et al.* [31] presented a new probe for PET/MRI formed by Mn-doped Fe_2O_4 (MnMEIO) with serum albumin conjugated with ^{124}I. In 2011, a different probe for the multimodal imaging PET/MRI was presented by Uppal *et al.* [32]; this probe was created combining Gd and ^{64}Cu to evaluate fibrin imaging effect on rats. Yang *et al.* [33] demonstrated a drug delivery function for tumor application combining a tracer for MRI with a ^{64}Cu and a drug (doxorubicin) conjugating them to SPIONs. In 2013, de Rosales [16] described the use of cocktails of imaging agents and bimodal agents to acquire information by PET/MRI technique, and he presented a probe (SPIONs) conjugated with ^{64}Cu. An important characteristic of the presented literature studies is the use of radiopharmaceuticals which have a very high half-life and are not utilized in the clinical practice for their higher radioactive power.

Recently, we have developed an efficient way based on a modified complex coacervation and double cross-linking reaction to produce hybrid core shell nanoparticles (HyCoS NPs) with improved relaxometric properties and able to increase the relaxivity of the clinically relevant Gadolinium-based Contrast Agents up to five-times without their chemical modification [34]. Here, the same HyCoS probe is presented, and its stability to a protocol of sorption of the fluorodeoxyglucose (^{18}F-FDG) is reported to be used as a tracer for integrated PET/MRI acquisitions. The radiopharmaceutical compound ^{18}F-FDG is selected together with the Gd-DTPA because they are the most commonly used in clinical practice for different kinds of diseases, potentially enabling the easy translation of our designed probe in clinical practice.

Materials

Chitosan (Ch) low molecular weight; divinyl sulfone (DVS) 118.15 g/mol; sodium tripolyphosphate (TPP) 367.86 g/mol; glacial acetic acid molecular weight 60.05; ethanol (EtOH) molecular weight 46.07; Gd-DTPA molecular weight 547.57; mineral oil 0.84 g/ml at 25°C; Span80 molecular weight 274.43; 1.005 g/ml at 20°C are purchased by Sigma-Aldrich®, while hyaluronic acid (HA) 850 kDa parenteral grade is by Hyasis. MilliQ water is for all experiments. ^{18}F-FDG (0.014 mg/ml) is synthesized and provided by IRCCS SDN of Naples.

Methods

Preparation of HyCoS NPs & their collection

As reported in a previous work, Vecchione *et al.* [34], HyCoS-NPs are produced through a complex coacervation process to obtain a core-shell architecture. Briefly, the HyCoS NPs are composed of a Chitosan core and a shell of HA. First of all, a w/o emulsion is prepared to obtain the core template. A total of 50 ml of a solution of mineral oil at 1% v/v Span80 is homogenized at 7000 r.p.m. for 5 min. Then, an acetic acid (AcOH) solution (34.93 mM) at 1% w/v Ch and 1% w/v Gd-DTPA is added to the previous oil solution and homogenized for 20 min at 7000 rpm to obtain a w/o nanoemulsion. Consequently, a water solution at 30% w/v of TPP and 0.1% w/v of HA is added to the previous emulsion and homogenized at 7000 rpm for other 30 min. Then, the emulsion is kept under continuous stirring overnight at 300 rpm. NPs are then collected and purified to achieve a concentration from 3 to 5 mg/ml.

Characterization of HyCoS NPs

A field emission scanning electron microscope (FE-SEM) by Zeiss transmission electron microscope (TEM) by FEI® in DRY, CRYO and tomography (TOMO) modes, are used to characterize the system morphologically. The SEM observations are made by collecting NPs on an ISOPORE membrane of 100 nm pore size. NPs are coated with 7 nm Au or Pt/Pd prior observation. The TEM analyses are conducted both in

DRY, CRYO and TOMO modes. In the DRY mode, 20–40 µl of NPs are collected on a Formvar/Carbon 200 mesh Cu, Agar. In CRYO mode, the samples are prepared using VITROBOT FEI coating Lacey Carbon film 200 mesh Cu Agar with 3 µl of NPs suspension under vitrification conditions of blotting time 1 s, humidity upper than 70% and temperature 20°C.

Synthesis of ^{18}F-FDG

The radiotracer ^{18}F-FDG is directly produced and used in the laboratories of the Diagnostic Center IRCCS SDN located in Naples. The chemical form of the ^{18}F is [^{18}F] fluoride ion, and it is produced by a cyclotron. Once the bombardment is complete, the radioactive solution containing the [^{18}F] fluoride ion is transferred from the target to the chemistry processing module where the reaction with the glucose for the formation of ^{18}F-FDG occurs. Usually, a whole batch of ^{18}F-FDG is dedicated to the testing of the NPs for each experiment.

Protocol of absorption of ^{18}F-FDG into HyCoS NPs loading Gd-DTPA

Absorption of decayed ^{18}F-FDG

Protocol of absorption is preliminarily assessed by using decayed ^{18}F-FDG at the IIT@CRIB Laboratories. During this preliminary test, different parameters of sorption have been studied (volume ratio and time of contact between HyCoS NPs and FDG, stirring rate regarding rpm and vacuum pressure to perform ultrafiltration, etc.). After ultrafiltration and purification steps, mass spectrometry (Agilent Technologies 6530 Accurate-Mass Q-TOF LC/MS, USA) is used to measure the amount of decayed ^{18}F-FDG loaded into the NPs. Furthermore, a release profile in phosphate-buffered saline of the NPs is studied by dialysis. A total of 100 µl of the phosphate-buffered saline washing phase are collected every 10 min up to 12 h and replaced with fresh medium. The release profile is assessed by mass spectroscopy.

Absorption of radioactive ^{18}F-FDG

The protocol of absorption of the radioactive tracer is directly conducted at the Radiopharmaceutical Department of the Diagnostic Center IRCSS SDN in Naples. Here, 100–500 µl of a solution ^{18}F-FDG at 0.014 mg/ml and about 60 µCi/ml (t_0) are added at different ratio to 100–500 µl of Gd-loaded NPs at a concentration of 1–5 mg/ml. The suspension is kept under continuous shaking for 5–10 or 20 min. This procedure is repeated at least four-times for at least four batches to achieve the required clinical administration dosage. Later, 1–3 ml of milliQ water are added to all the batches, and put under vacuum to perform ultrafiltration (30 s) through an adapted Concentrator Corning Disk (SPIN-X UF 30 kDa of 20 ml by SIGMA) enabling the controlled separation of not adsorbed radiotracer from the HyCoS NPs. Both the solution of water and the residual ^{18}F-FDG, and the suspension of NPs are then collected in different tubes to measure their activities.

Simultaneous PET/MRI acquisition

After the protocol of sorption, the radioactive HyCoS NPs are collected and injected into each fillable sphere (inner diameters: 10 mm (A), 13 mm (B), 17 mm (C), 22 mm (D), 28 and 37 mm) of a specific NEMA 2012/IEC NEMA IEC Body Phantom (Figure 1); the phantom is placed at the isocenter of the PET/MR field of view to perform simultaneous PET/MRI acquisition. The eluates of the related samples are also measured to assess the efficacy of the sorption. The images of radiotracer distribution, as well as MR T1-weighted sequence of bimodal contrast agent, were simultaneously obtained by a PET/MRI scan.

In vitro MRI

Relaxation times of the Gd-loaded NPs are measured on a Bruker Minispec (mq 60) bench-top relaxometer operating at 60 MHz for protons (magnetic field strength: 1.41 T). The acquisitions are performed at 37°C. Before each measurement, the sample is placed into the nuclear magnetic resonance probe for about 15 min for thermal equilibration. Longitudinal relaxation times, T_1, is determined by both saturation (SR) and inversion recovery pulse sequences. Relaxivity values, r_1, are calculated from the slope of the regres-

Figure 1. Image of the specific phantom utilized to perform PET/MRI acquisition of hybrid core shell nanoparticles. The low volume glass burettes are filled with a selected sample at a specific concentration.

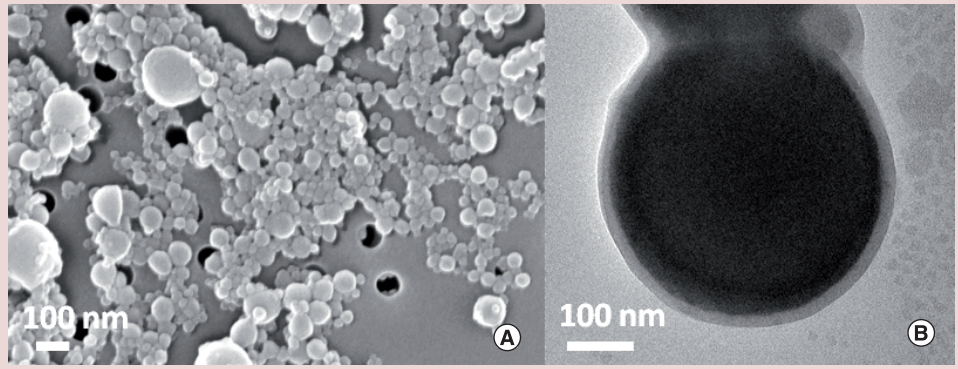

Figure 2. Morphological characterization. (A) SEM image of HyCoS NPs and **(B)** TEM image of core-shell HyCoS NPs.
HyCoS NP: Hybrid core shell nanoparticle; SEM: Scanning electron microscope; TEM: Transmission electron microscope.

sion line of $1/T_1$ [s^{-1}] versus concentration [mM] with a least-squares method using Origin Pro 9.1 SRO software (OriginLab Corporation, MA, USA). For the correct evaluation of the r_1, Gd concentration of the NPs' suspension is ranged between 0 and 100 µM to evaluate r_1 avoiding the contribution of the T_2 effects.

Results

The morphology of the HyCos NPs is characterized by SEM and TEM microscopy. In the following figure (Figure 2) are reported an SEM image and a TEM image of the NPs. Figure 2A highlights the spherical NPs while the Figure 2B shows the core-shell architecture of the designed NPs.

The size of the NPs will play an important role in the biodistribution of the carries and in the accumulation at a different time and different organs. However, currently, the selection of an appropriate architecture is able to deliver more than one tracer simultaneously, and eventually being a theranostic tool is the first step for the design of an effective multimodal probe.

Evaluation of the encapsulation efficiency of the decayed ^{18}F-FDG absorbed by NPs & their stability

A calibration line of glucose (range 0–0.014 mg/ml) used for the evaluation of the concentration of decayed ^{18}F-FDG by mass spectroscopy is shown.

After the contact and the purification protocols, a decayed ^{18}F-FDG concentration of 0.00325 mg/ml is measured on the flow-through collected at the bottom of the flask. The difference between the residual product and the initial amount of used ^{18}F-FDG is reported in Table 1 and shows the quantity absorbed into the NPs.

Protocol of sorption

In the design of a process that should be integrated into an industrial and certificated quality system, currently in use in radiopharmaceutical laboratories for the development of a new multimodal probe, the first endeavor was to integrate the production of polymeric NPs with the synthesis of ^{18}F-FDG. Indeed, the starting idea was to encapsulate the glucose during the manufacturing process of the NPs and to perform, later, directly in the hot cell, the substitution of the oxygen with the ^{18}F within the NPs. Unfortunately, the synthesis of ^{18}F-FDG (Figure 3), such as the others radiopharmaceutical tracers, is conducted at a temperature profile (104°C) not suitable for polymeric materials, causing the instability of the NPs. Furthermore, beyond the difficulties related to the stability of the NPs, even the quality controls of the ^{18}F-FDG were compromised by this procedure while our aim is

Table 1. Mass spectrometry: measures are made on eluate after a purification step of the particles.

NPs (µl)	FDG 0.014 mg/ml (µl)	Initial amount of FDG (mg/ml)	Destruction of the integrity of the NPs	Residual amount of FDG (mg/ml)	Difference (mg/ml)	Sorption (%)
500	100	26.283E-13	Yes	ND	ND	ND
500	10	26.283E-13	No	1.02715E-13	1.60115E-13	61

The results show a sorption of about 60% of the FDG after the contact of 10 min with the NPs.
FDG: Fludeoxyglucose; ND: Not determined; NP: Nanoparticle.

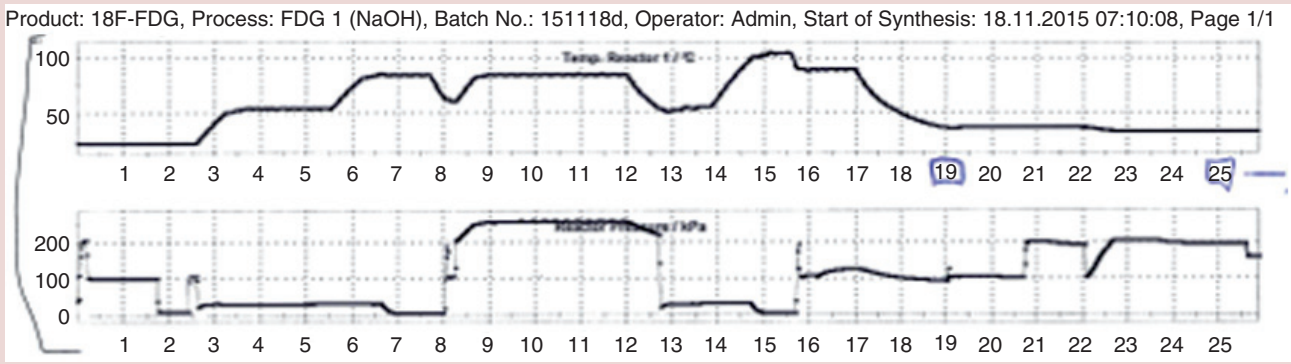

Figure 3. Acquired profile of pressure and temperature during the ^{18}F-FDG synthesis.

to improve the diagnostic without the chemical modification of the approved compounds. In this perspective, the production of a polymeric NP in the hot cells is not effective and extremely expensive. The second strategy we have carried out regards the combination of the ^{18}F-FDG with the polymeric NPs by absorption of the radiotracer. In details, after their production, HyCoS NPs are subjected to freeze-drying to remove the excess water before keeping in contact the materials as described in the Materials and Methods sections. An experimental campaign was conducted to estimate the conditions of sorption regarding the preservation of the shape of the NPs and encapsulation efficiency of the ^{18}F-FDG. The optimal conditions are obtained by adding 100 µl of a solution ^{18}F-FDG, at 0.014 mg/ml, at 60 µCi/ml (t_0), to 500 µl of NPs. NPs' suspension used for the sorption had a concentration of 1 mg/ml, a Gd concentration of 150 µM, a T_1 = 300 ± 20 ms (T_1 equal to 750 µM of unloaded Gd-DTPA). Formed suspension is kept under continuous shaking for 10 min. Later, 1 ml of milliQ water is added to all the batches, and put under vacuum to perform ultrafiltration.

Figure 4 reported an SEM image of NPs after the protocol of sorption with decayed ^{18}F-FDG. The image clearly shows that the NPs maintain their shape after the protocol of absorption if it is performed at the

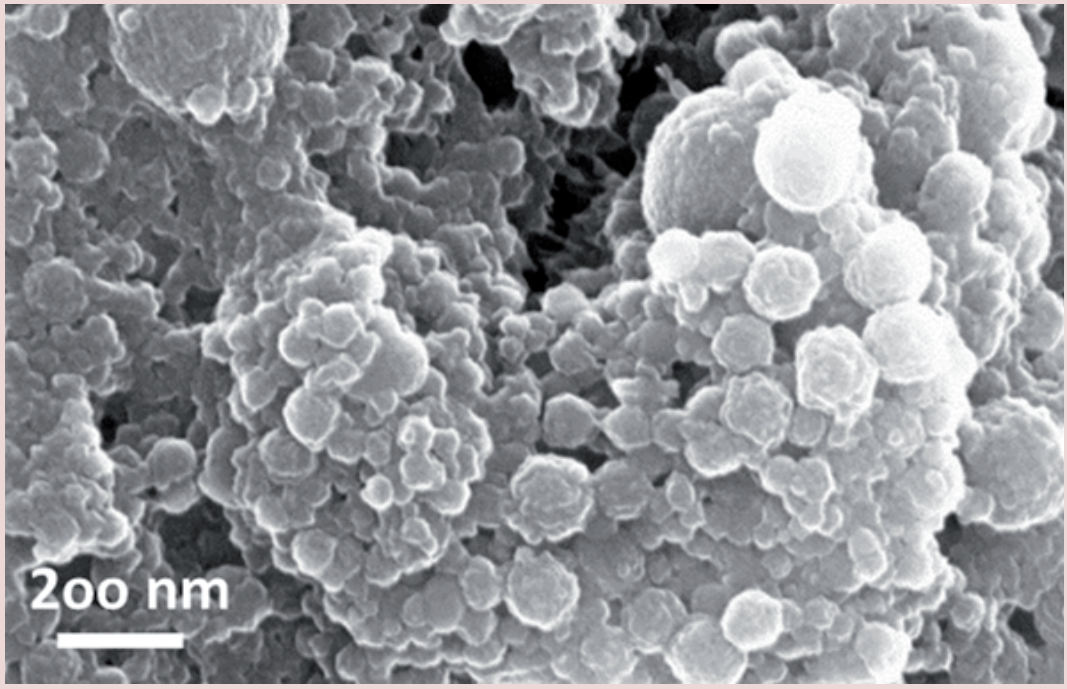

Figure 4. Morphological characterization of nanoparticles by field emission scanning electron microscope.
Nanoparticles with Gd-DTPA after the sorption step performed with ^{18}F-FDG decayed at 0.014 mg/ml.

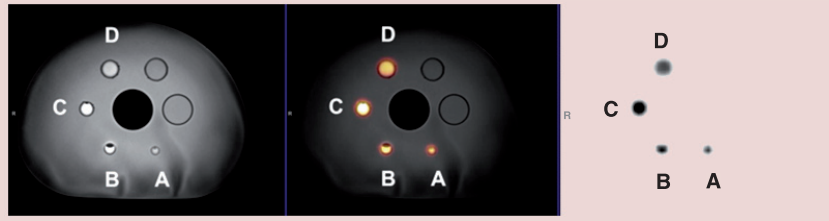

Figure 5. Simultaneous PET/MRI acquisition: on the left: the MR scan; in the middle: PET/MR fusion; on the right: only PET observation.

selected optimal conditions. At these conditions, the improved relaxometric properties of the loaded Gd-DTPA are also preserved and the release of the radiotracers is detected only after 8 h.

In vitro simultaneous PET/MRI acquisition

Figure 5 shows the images resulting from the simultaneous PET/MR acquisition. The co-registration PET/MRI (Figure 5, middle) of the signals on the samples do not present interference, enabling the measurements of a T_1 equal to 300 ms (Figure 5, right A) and 600 ms (Figure 5, right B) and the PET in a range between 1.87 (Figure 5, middle A) and 3.32 µCi (Figure 5, middle B), 90 min after the synthesis of ^{18}F-FDG (60 µCi/ml). The analysis of the radioactivity performed on the eluates (Figure 5, right C & D) showed an activity of about 6 µCi at the same time point (Figure 5, middle C & D). The time point for the measurement is selected taking into account the half-life of the radiotracer (about 1 h). Results show that the amount of radiotracers absorbed by the HyCoS NPs is sufficient to obtain a human administration dosage. Furthermore, MRI analysis in samples at different concentration is reported in Figure 6. The slope of the line related to the linear regression represents the relaxivity r_1 of the contrast agents. The plot shows a relaxivity r_1 equal to 4 for the commercial 'free Gd-DTPA' and to 21 for the HyCoS NPs entrapping the Gd-DTPA. Equation assessed a boosted relaxivity r_1, on an MRI 3 Tesla, of about five-times compared with the free Gd-DTPA (Figure 6) even after the protocol of sorption. As previously reported, the concentration of the Gd-loaded NPs is ranged between 0 and 100 µM to avoid artifacts due to T_2 effects.

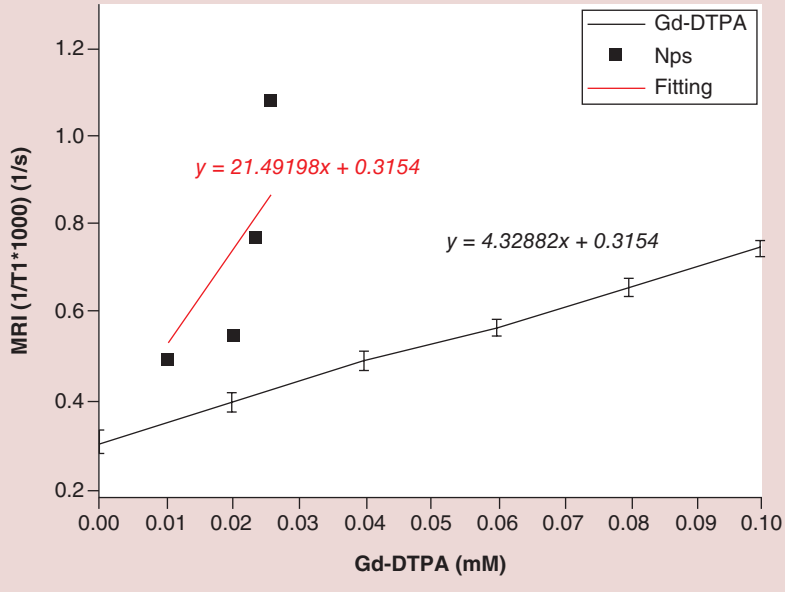

Figure 6. *In vitro* MRI. Longitudinal relaxation rate as a function of (Gd-DTPA) concentration for: Gd-DTPA in distilled water at different concentrations (lower line); HyCoS NPs loaded with Gd-DTPA at different concentration (upper line); Linear regression is performed for each system, and related equations are showed.
Gd-DTPA: Gadopentetic acid; HyCoS NP: Hybrid core shell nanoparticle.

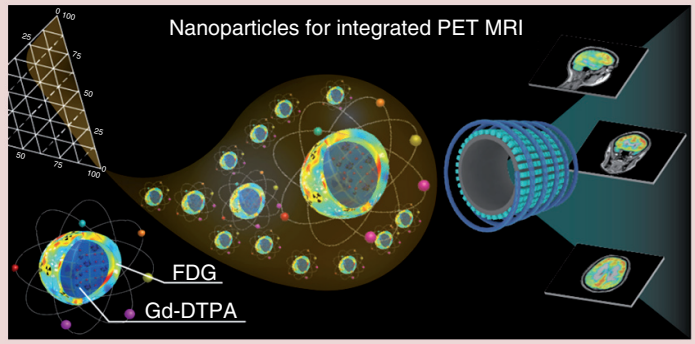

Figure 7. Graphical representation of future perspectives of hybrid core shell nanoparticles for integrated PET/MRI.
FDG: Fludeoxyglucose; Gd-DTPA: Gadopentetic acid.

Discussion

The proposed protocol could be integrated at the downstream of the synthesis of ^{18}F-FDG. Indeed, the radiotracer can be entrapped into the NPs taking advantages by the positive charge of the chitosan core which can attract the radiotracer and control its release by sorption. Furthermore, using the method described in this chapter, it is possible to combine the designed nanovectors directly with the radiotracers, making the product available as a ready-to-use compound in the clinical practice. The sorption of the radiotracer within the NPs might be mainly due to the concentration gradient obtained by freeze drying between the external and the internal phases. However, the entrapment of the radiotracer should probably be attributed to the positive charge of the chitosan scorekeeping the radiopharmaceutical compound (negatively charged) trapped in the polymer mesh. Future *in vivo* studies will assess the stability and the biodistribution of the NPs. Indeed, it is important to point out that when the tracers are entrapped within NPs, it will follow their biodistribution. In details, the radiotracer will not follow the traditional metabolic pathway of the glucose but a new one dictated by the body clearance and interaction of the NPs. The protocol used enables preparing an injectable suspension usable for simultaneous acquisitions PET/MRI without altering the chemical nature of the molecules as approved by the FDA. In addition, the boosted relaxometric properties of the HyCoS NPs are also preserved, providing a probe with improved efficacy (Figures 5 & 6). The results show an enhancement in r_1 of about five-times compared with the free Gd-DTPA, due to the presence of the mixed hydrophobic-hydrophilic hydrogels [35].

Furthermore, it is important to point out that the formulation of the HyCoS NPs respects the amount of radiotracer, the metal chelates concentration and the acquisition window currently in clinical use. It represents a significant and unique result, paving the way to a new class of completely biocompatible probes with improved performances that could add notable development to the diagnostic field and the nanomedicine in general, with an effective exploitation of simultaneous hybrid imaging (Figure 7).

Conclusion

In conclusion, the HyCos NPs, encapsulated with Gd-DTPA for MRI in a previous work, have been dried to be able to absorb ^{18}F-FDG. A precise control of the components and the process parameters for the protocol of sorption was introduced to entrap efficiently ^{18}F-FDG for simultaneous PET/MRI applications without weakening the stability of the NPs and the release of the compounds. Indeed, using the proposed protocol, the HyCoS NPs preserve a boosting of the MRI signal and can absorb a detectable dosage of a radiotracer if opportunely treated.

The *in vitro* results performed on a PET/MRI scan have shown that the nanovectors improve the relaxometric properties and preserve the radioactivity without any chemical modification of the FDA-approved molecules. Furthermore, both the MR and the PET signals simultaneously acquired are not influenced by the presence of the polymer carrier.

Future development of this project will be the study of the biodistribution of the multimodal nanovectors to evaluate the stability of the complex and its biodistribution.

Acknowledgements

The authors gratefully acknowledge the graphic designer, V Latilla, for her contribution to the preparation of the graphical abstract, and V Mollo for her technical support to the characterization by TEM.

Financial & competing interests disclosure

The authors have no relevant affiliations or financial involvement with any organization or entity with a financial interest in or financial conflict with the subject matter or materials discussed in the manuscript. This includes employment, consultancies, honoraria, stock ownership or options, expert testimony, grants or patents received or pending, or royalties.

No writing assistance was utilized in the production of this manuscript.

Summary points

- This work aims to design and develop new polymeric nanovectors for simultaneous PET/MRI acquisitions.
- The Gd-DTPA and the fluorodeoxyglucose (^{18}F-FDG) are chosen respectively as a contrast agent for MRI and a radiotracer for PET imaging.
- The nanoparticles (NPs) are obtained by a modified complex coacervation process.
- The sorption protocol of the ^{18}F-FDG by the NPs is specifically designed to entrap the tracer itself in the NPs downstream the production process of the ^{18}F-FDG.
- *In vitro* PET/MRI analysis is made to evaluate the activity of the radiotracer absorbed by the NPs and the MR signal.
- Both the co-registred signals are simultaneously visible, and the PET signal is not negatively influenced by the presence of the polymer nanovector.
- The boosted relaxometric properties of the hybrid core shell NPs are also preserved improving the probe efficacy.
- The results show an enhancement in r_1 of five-times compared with the free Gd-DTPA.

References

Papers of special note have been highlighted as: • of interest; •• of considerable interest

1 Drzezga A, Souvatzoglou M, Eiber M *et al.* First clinical experience with integrated whole-body PET/MR: comparison to PET/CT in patients with oncologic diagnoses. *J. Nucl. Med.* 53(6), 845–855 (2012).

2 Pichler BJ, Kolb A, Nagele T, Schlemmer HP. PET/MRI: paving the way for the next generation of clinical multimodality imaging applications. *J. Nucl. Med.* 51(3), 333–336 (2010).

3 Judenhofer MS, Wehrl HF, Newport DF *et al.* Simultaneous PET-MRI: a new approach for functional and morphological imaging. *Nat. Med.* 14(4), 459–465 (2008).

•• **It gives a technical overview of the PET-MRI approach, exploiting the advantages of the simultaneous approach.**

4 Salerno M, Porqueras DSD. Alzheimer's disease: the use of contrast agents for magnetic resonance imaging to detect amyloid beta peptide inside the brain. *Coord. Chem. Rev.* 327, 27–34 (2016).

5 Pagel MD. The hope and hype of multimodality imaging contrast agents. *Nanomedicine* 6(6), 945–948 (2011).

6 Pimlott SL, Ebmeier KP. SPECT imaging in dementia. *Br. J. Radiol.* 80, S153–S159 (2007).

7 Jack CR. Alzheimer disease: new concepts on its neurobiology and the clinical role imaging will play. *Radiology* 263(2), 343–360 (2012).

8 Catana C, Drzezga A, Heiss W-D, Rosen BR. PET/MRI for neurologic applications. *J. Nucl. Med.* 53(12), 1916–1925 (2012).

• **PET-MRI is a relevant technique for application in brain pathologies. This work gives an overview of the application at neurological diseases.**

9 Yankeelov TE, Peterson TE, Abramson RG *et al.* Simultaneous PET-MRI oncology: a solution looking for a problem? *Magn. Reson. Imaging* 30(9), 1342–1356 (2012).

10 Small GW, Bookheimer SY, Thompson PM *et al.* Current and future uses of neuroimaging for cognitively impaired patients. *Lancet Neurol.* 7(2), 161–172 (2008).

11 Lee DE, Koo H, Sun IC, Ryu JH, Kim K, Kwon IC. Multifunctional nanoparticles for multimodal imaging and theragnosis. *Chem. Soc. Rev.* 41(7), 2656–2672 (2012).

12 Rousset OG, Ma YL, Evans AC. Correction for partial volume effects in PET: principle and validation. *J. Nucl. Med.* 39(5), 904–911 (1998).

13 Aiello M, Salvatore E, Cachia A *et al.* Relationship between simultaneously acquired resting-state regional cerebral glucose metabolism and functional MRI: a PET/MR hybrid scanner study. *NeuroImage* 113, 111–121 (2015).

•• **This cited work supports the previous overview reporting a study conducted on the brain by the hybrid PET-MRI scanner.**

14 Flory PJ. Fundamental principles of condensation polymerization. *Chem. Rev.* 39, 137–197 (1946).

15 Brechbiel MW. Bifunctional chelates for metal nuclides. *Q. J. Nucl. Med. Mol. Imaging* 52(2), 166–173 (2008).

16 De Rosales RTM. Potential clinical applications of bimodal PET-MRI or SPECT-MRI agents. *J. Labelled Comp. Radiopharm.* 57(4), 298–303 (2014).

17 Hahn MA, Singh AK, Sharma P, Brown SC, Moudgil BM. Nanoparticles as contrast agents for *in-vivo* bioimaging: current status and future perspectives. *Anal. Bioanal. Chem.* 399(1), 3–27 (2011).

18 Utech S, Boccaccini AR. A review of hydrogel-based composites for biomedical applications: enhancement of hydrogel properties by addition of rigid inorganic fillers. *J. Mater. Sci.* 51(1), 271–310 (2016).

• **An overview of the properties of the hydrogels partially applied to this process.**

19 Frullano L, Catana C, Benner T, Sherry AD, Caravan P. Bimodal MR-PET agent for quantitative pH imaging. *Angew. Chem. Int. Ed. Engl.* 49(13), 2382–2384 (2010).

•• **An application of PET/MRI to pH responsive agents, proving the added value of this instrumentation for the acquisition of further information.**

20 Kiani A, Esquevin A, Lepareur N, Bourguet P, Le Jeune F, Gauvrit JY. Main applications of hybrid PET-MRI contrast agents: a review. *Contrast Media Mol. Imaging* 11(2), 92–98 (2016).

21 Lin J, Chen XY, Huang P. Graphene-based nanomaterials for bioimaging. *Adv. Drug Del. Rev.* 105, 242–254 (2016).

22 Garcia J, Tang T, Louie AY. Nanoparticle-based multimodal PET/MRI probes. *Nanomedicine* 10(8), 1343–1359 (2015).

•• **A relevant overview of the attention dedicated to the design of new probes for the multimodal imaging.**

23 Yang BY, Kim YI, Moon SH *et al.* Development of PET/MRI imaging probes using facile encapsulation methods with specially designed amphiphiles. *J. Nucl. Med.* 55, 1 (2014).

24 Blasiak B, Van Veggel F, Tomanek B. Applications of nanoparticles for MRI cancer diagnosis and therapy. *J. Nanomaterials* 2013, 148578 (2013).

25 Kawai T, Rahman N, Matsuba G *et al.* Crystallization and melting behavior of poly (L-lactic acid). *Macromolecules* 40(26), 9463–9469 (2007).

26 Lux F, Sancey L, Bianchi A, Cremillieux Y, Roux S, Tillement O. Gadolinium-based nanoparticles for theranostic MRI-radiosensitization. *Nanomedicine* 10(11), 1801–1815 (2015).

27 Cisneros BT, Law JJ, Matson ML, Azhdarinia A, Sevick-Muraca EM, Wilson LJ. Stable confinement of positron emission tomography and magnetic resonance agents within carbon nanotubes for bimodal imaging. *Nanomedicine* 9(16), 2499–2509 (2014).

28 Okumura M, Mikawa M, Yokawa T, Kanazawa Y, Kato H, Shinohara H. Evaluation of water-soluble metallofullerenes as MRI contrast agents. *Acad. Radiol.* 9, S495–S497 (2002).

29 Lee HY, Li Z, Chen K *et al.* PET/MRI dual-modality tumor imaging using arginine-glycine-aspartic (RGD)-conjugated radiolabeled iron oxide nanoparticles. *J. Nucl. Med.* 49(8), 1371–1379 (2008).

30 Hwang DW, Ko HY, Lee JH *et al.* A nucleolin-targeted multimodal nanoparticle imaging probe for tracking cancer cells using an aptamer. *J. Nucl. Med.* 51(1), 98–105 (2010).

31 Zhu H, Zhao J, Lin XF, Hong Y, Li C, Yang Z. Design, synthesis and evaluation of dual-modality glyco-nanoparticles for tumor imaging. *Molecules* 18(6), 6425–6438 (2013).

32 Uppal R, Catana C, Ay I, Benner T, Sorensen AG, Caravan P. Bimodal thrombus imaging: simultaneous PET/MR imaging with a fibrin-targeted dual PET/MR probe-feasibility study in rat model. *Radiology* 258(3), 812–820 (2011).

33 Yang XQ, Hong H, Grailer JJ *et al.* cRGD-functionalized, DOX-conjugated, and Cu-64-labeled superparamagnetic iron oxide nanoparticles for targeted anticancer drug delivery and PET/MR imaging. *Biomaterials* 32(17), 4151–4160 (2011).

34 Vecchione D, Grimaldi AM, Forte E, Bevilacqua P, Netti PA, Torino E. Hybrid Core-Shell (HyCoS) nanoparticles produced by complex coacervation for multimodal applications. *Sci. Rep.* 7, 45121–45121 (2017).

•• **The methodology applied to obtain the hybrid core shell nanoparticles used in this work as PET/MRI probe.**

35 Ponsiglione AM, Russo M, Netti PA, Torino E. Impact of biopolymer matrices on relaxometric properties of contrast agents. *Interface Focus* 6(6), 20160061 (2016).

•• **Reports a fundamental understanding of the principles relating to the boosting of relaxametric properties of Gd-based contrast agents in the hydrogel matrix.**